Original Research Article



Lifestyle Cost-Effective Strategies for Tamsulosin HCl Extended-Release Tablets Using Polymer Mixtures for Solubility Improvement

Kashif Barkat¹, Umair IKram Dar², Anaum Asghar³, Hira Shahid⁴, Nariman Shahid¹, Rabia Arshad¹, Zeeshan Akbar¹, Shamsha Kanwal⁵, Hamza Rafeeq⁶, Haroon Yousaf¹

¹Faculty of Pharmacy, The University of Lahore, Pakistan|²College of Pharmaceutical Sciences, Lahore, Pakistan|³Faculty of Pharmaceutical Sciences, University of Central Punjab, Lahore, Pakistan|⁴Department of Pharmacology, Faculty of Pharmaceutical Sciences, Government College University, Faisalabad, Pakistan|⁵Department of Biochemistry, University of Agriculture, Faisalabad, Pakistan|⁶Department of Biochemistry, Riphah International University, Faisalabad, Pakistan

Correspondence should be addressed to Kashif Barkat; dr.kashif2009@gmail.com

Received: 11 April 2025; Revised: 23 June 2025; Accepted: 26 July 2025; Published 26 September 2025

KEYWORDS

Tamsulosin HCl Matrix Dissolution Cashew gum Formulations

ABSTRACT

The present research was designed to investigate the extraction, purification, and characterization of cashew gum, as well as its combination with HPMC and xanthan gum, in pharmaceutical applications. In this research, we prepared ten formulations by varying the quantity of cashew gum. The cashew gum recovery rate from the purifying procedure was 72.26%. The viscosity, swelling index, particle size distribution, and bulk density of cashew gum were determined, along with several physical, rheological, and flow characteristics that were examined. The use of these gums, along with HPMC and xanthan gum, in the production of Tamsulosin HCl matrix tablets was also investigated in this study. To assess the tablets' performance, quality control tests were carried out, including weight uniformity, friability, crushing strength, swelling index, and dissolution investigations. According to regulatory requirements, some formulations produced sustained drug release over 24 hours, as shown by the release kinetics and drug dissolution profiles. To evaluate the reliability and compatibility of the excipients, characterization methods including X-ray diffraction (XRD), differential scanning calorimetry (DSC), thermogravimetric analysis (TGA), and Fourier transform infrared spectroscopy (FTIR) were used. FTIR spectra show different peaks of functional groups. Scanning Electron Microscopy analysis shows that the tablet surface was porous. The results show that cashew gum is a good substitute for a pharmaceutical excipient that might be used in formulations for controlled drug release.

Copyright © 2025 Kashif Barkat et al. is an open-access article distributed under the Creative Commons Attribution License, which permits use, distribution, and reproduction in any medium, provided the original work is properly cited.

1. Introduction

Lower urinary tract symptoms (LUTS), which are indicative of benign prostatic hyperplasia, involve the enlargement of the prostate gland and affect approximately 25% of men in their 50 s, 33% of those in their 60 s, and 50% of all men in their 80 s or older. The prostate gland encircles the urethra, and its progressive enlargement with age can exert pressure on the urethral lumen, often leading to compromised urinary function. This age-associated condition, benign prostatic hyperplasia (BPH), develops in nearly all aging men and, though nonneoplastic in nature, presents bothersome urinary symptoms. Epidemiological data indicate that approximately 50% of men over the age of 75 exhibit clinical manifestations of BPH. Its severity escalates with age and is frequently associated with comorbidities such as cardiovascular disease, hypertension, erectile dysfunction, and urinary retention. In addition to bladder and urethral involvement, prostate pathology significantly contributes to urinary dysfunction. Consequently, the term "prostatism" has been replaced with the broader, pathophysiological, inclusive term "lower urinary tract symptoms" (LUTS) (McVary et al,2014). LUTS are prevalent among older adults and show considerable interindividual variability, both temporally and geographically, often defying uniform explanation. The rising prevalence of BPH, coupled with growing therapeutic demand, is expected to elevate the overall healthcare burden. This trend persists despite pharmacotherapy potentially reducing the need for surgical interventions. The economic impact on individual patients remains a key determinant in shaping the adoption of long-term pharmacological regimens. While urinary symptom improvement drives therapeutic flexibility, the clinical significance of this benefit remains under scrutiny, as conclusive evidence from controlled studies is limited. Currently, approximately 80% of clinicians initiate treatment using alpha-1 adrenergic receptor antagonists. Since its introduction in 1997, tamsulosin has been widely prescribed in the United States due to its receptor selectivity, minimal interaction with antihypertensive agents, and a low incidence of cardiovascular adverse events. It represents the first pharmacological agent specifically engineered to target both BPH and associated urinary tract symptoms. However, the modified-release capsule formulation of tamsulosin presents pharmacokinetic challenges (Kava BR et al, 2019). When administered in the fasting state, it yields a 30% increase in systemic exposure and a 70% elevation in peak plasma concentration. This variability contributes to a higher incidence of adverse effects, a

limitation often exacerbated by the capsule dosage form. An optimized approach involves reformulating tamsulosin into a sustained-release tablet, enhancing the therapeutic index and patient compliance. A once-daily dosing schedule ensures more consistent plasma drug levels and aligns with the circadian rhythm of pharmacodynamics. Moreover, in vivo drug release from the tablets demonstrated favorable pharmacokinetic behavior under fasting and controlled conditions, although plasma concentrations were notably influenced by concurrent food intake. This could be because the pills stay in the proximal parts of the intestine for a long time, which causes slow drug absorption and very high peak plasma concentrations (Rivera-Navarro, Pizaño et al. 2024). According to the study, increased plasma peak medication concentrations occur following the consumption of long-lasting formulations combined with food. It is possible to explain improper mixing in the stomach's proximal region, which is notis not always caused by an issue with the opioid release control formulation (Holanda, Oliveira et al. 2024).

To enhance drug release kinetics and improve patient compliance, this study aims to develop and evaluate a sustained-release matrix tablet of tamsulosin hydrochloride using natural polymers, specifically cashew gum, in conjunction with established excipients such as HPMC and xanthan gum. A release-controlling agent, microcrystalline cellulose (Avicel), and Tamsulosin are among the several pulverised components used in the modified-release dosage form. Ultimately, these granules enable the pulverized matrix to release Tamsulosin in a controlled manner. Avicel provides structural support, while cross-carmellose sodium binds the granular units together and regulates their release; inert excipients make up the matrix system. Tamsulosin is the active ingredient. A stable and effective final dose form is created by compressing the resultant granulate. This form is intended for , more extended drug release (Ofori-Kwakye et al).

2. Materials and methods

2.1. Material Collection

Tamsulosin Hydrochloride was gifted from Everest Pharmaceuticals, Islamabad. Hydroxypropyl methylcellulose (HPMC), xanthan gum, Avicel, PVP K30, croscarmellose sodium, starch, stearate, microcrystalline cellulose, and talc were all acquired from the University of Lahore's Department of Pharmaceutics' Chemical Store.

Table 1: Ratios of polymers used in the formulations

Formulation	Tamsulosin Hydrochloride	Cashewgum (g)	HPMC (g)	Xanthangum (g)
F-1	0.0004 g	0.5		0.5
F-2	0.0004 g	1.0		0.5
F-3	0.0004 g	1.5		0.5
F-4	0.0004 g	2.0		0.5
F-5	0.0004 g	2.5		0.5
F-6	0.0004 g	0.5	0.5	
F-7	0.0004 g	1.0	0.5	
F-8	0.0004 g	1.5	0.5	
F-9	0.0004 g	2.0	0.5	
F-10	0.0004 g	2.5	0.5	

2.5. Rheology of cashew gum

Purified water was used to treat the mucilage in different concentrations of cashew gum (1% w/v, 2% w/v, 5% w/v, and 10% w/v). A Bradford viscometer (spindle number 2) was used to measure

Cashew gum was extracted in the lab of the university. The rest of the chemicals used in this research were of laboratory grade.

2.2. Preparation and Refinement of Cashew Gum

By hand-grabbing, breaking, and filtering bark and other external elements, the crude cashew gum was purified. For roughly ten hours, the gum was dried at 60 °C in an oven until it became too brittle. After that, the dried gum is separated into light and dark grades. After being melted into a fine powder in a porcelain mortar, the light-colored material was chosen for additional processing. The gum has been utilized as raw gum powder. 700 g of the crude gum powder was mixed with 1400 ml of filtered water to purify it and left for 24 hours (Ola, Emikpe et al. 2024). With a sheet of calico, the gum adhesives are ground away to remove any decay or insoluble waste. The sift adhesive has been re-separated. Ninety-six percent ethanol was used to purify the separate adhesive. After that, 700 g of gum, and dissolved in approximately 2500 ml of 96% ethanol. The gum was then sifted, cleaned with diethyl ether, and dried in a hot air oven set at 60 °C for about 8 hours. The 80 sifters have been used to treat and tame the dry filtered gum. In further studies and research, the powdery gum was employed as a wash for cashews (Aboul-Enein, Hussein et al., 2003).

2.3. Preparation of granules

The percentage of the polymer in each sample is shown in Table 1. Ten (10) different batches of granules were made using the wet granulation procedure. Tables 2 to 16 of the substances used show the precise amounts. The Retsch instrument was used to regulate the molecular size and circulation of cashew gum and xanthan powder. The electric shaker and Sifters' housing were located between Strainers 8 and 200. After applying 120 grams of rubber powder, the surface was sifted through the biggest sieve. After 15 minutes of shaking the powder at 60°, the volume of the powder in each sifter was weighed and recorded. Furthermore, the outcomes were subsequently applied (Ofori-Kwakye, Obese et al. 2013).

2.4. Compression of tablet

Each sustained-release tablet contained 0.4 mg of tamsulosin hydrochloride. Ten distinct batches were compressed using the single-punch tableting device, which featured concave punches and die collection. In a metal tray, the granules were placed shortly before the tension. Each party received a pill weighing 420 mg (Pawar, Jaimini et al. 2014).

the sample viscosities at a shear rate of 1 rpm (Malabadi, Kolkar et al 2021).

2.6. Flow curves of granules

Using a funnel, weigh 10 g of the gum in a 100 ml cylinder. To gather all the particles adhering to the cylinder wall, the cylinder was gently taped twice. The initial volume was recorded. On a wooden benchtop, Vf, the cylinder was struck 100 times from a height of 2 cm in order to obtain consistent volume readings. The initial bulk density, also known as Df, or mass/Vo, fluff, or bulk density, was computed as the initial bulk density. The ultimate bulk density, also known as Df, or mass/Vf, was occasionally measured. The Hausner ratio was determined to be the Df/Do ratio.

2.7. Angle of repose

The point of rest was also determined using the fixed stature measure. To form a cone, the gum was let run freely from the channel at a set height onto a level surface. The height of the pipe hole from the level surface was also determined, and the cone bottom was indicated. They calculated the cone's height. The formula $\tan = h/r$ was used to determine the center of rest based on the cone's height and the width of its midsection (Gopaiah, 2022).

2.8. Swelling capacity of granules

A 100 mL measuring chamber was filled with a 10 g sample of the gum, which was then repeatedly tapped. Next, the volume (V1) was recorded. To reach the 100 ml imprint, refined water was poured into the bulk, and it was then allowed to sit for a whole day. In the estimating chamber, the gum's new volume (V2) was noted. The ratio of the final volume to the gum's underlying volume was used to calculate the growth limit. Phosphate cushion, pH 7.5, was used as the expanding medium as the test proceeded (Fosu, Ofori-Kwakye et al. 2016).

2.9. Particle size analysis of Granules

The house of sifters was mastered from sieve 8 to sieve 200 using a mechanical shaker, and the Retsch Shaker was used to control the particle size distribution of cashew gum powder and xanthan. After weighing 110–120 g of gum powder, it was placed on the highest sieve and sealed with the top. The amount of powder kept on every sifter was measured and recorded after the powder was disturbed for 15 minutes at a vibrational frequency of 60°. The results were then applied to other counts.

2.10. Consistency of weight test

Twenty tablets were randomly selected from each lot, weighed, and then gauged separately. The weight of each tablet was subtracted from its average load, and the rate difference of each tablet from the average was fixed (Tafere, Yilma et al. 2021).

2.11. Crushing strength of tablets

With a Monsanto pill hardness tester, the crushing ability of the tablets was determined by diametral compression at room temperature. Ten tablets were selected at random from the many batches of tablets that were packed and utilized in the experiment. A tablet was positioned between the analyzer's plate and handle unfavorably until contact was established, at which point there was enough pressing force due to more screwing to cause breaking. After considering the size of the analyzer, the hardness was examined. Tablets that clearly split into equal sections without any sign of overlay were used to obtain distinct results. Every estimate was done in three steps.

2.12. Friability test of tablets

After dedusting and weighing a variety of tablets weighing more than 6 g (Wo), they were put on the Erweka Friabilator reservoir. After 25 minutes, the drum rotated and smashed the tablets, and the machine shut off. The tablets were inspected for cleavages, breakages, and cracks, and their final weight, Wf, was recorded. The percentage of weight loss was calculated.

Friability = Initial weight of tablets - final Weight of tablets x 100
Initial weight of tablets

2.13. Swelling index of tablets

The expanding list of tablet designs was taken into consideration. The percentage of weight gained by the tablet was used to measure the degree of growth. One pill from each detail was stored in a petri dish with 20 ml of pH 7.5 phosphate cushion. The tablet was using a tissue paper, and measured at the end of the hour. The procedure was then carried out for eighteen hours, with the pill weights being recorded every two hours. The weight gain percentage of the pills was calculated as follows:

% SI = Weight of swollen tablet – Initial weight of tablet x 100
Initial weight of tablet

2.14. Dissolution testing

In the six jars of the dissolution unit, the USP system II uses 900 milliliters of the dissolution medium (phosphate, pH 7.5). The paddle's speed was adjusted to 50, and the dissolution media was set up at $37\pm0.5\,$ °C. Every machine vessel had a tablet installed and ran at the designated pace. Five, fifteen, thirty, one, two, four, six, eight, ten, twelve, fifteen, eighteen, twenty-one, and twenty-four hours are the time cycles (Nanjwade, Ali et al. 2010). A sample was removed 10 mL from 1 cm at the vessel divider. The vessels were covered for the duration of the test, and the medium temperature was maintained at 37 \pm 0.5 °C consistently. The dried-out models had been separated using the Whatman paper.

After removing the 10 mL test sample, 10 mL of fresh separating medium was added to the vessel, after which the volume was removed. A 1 cm cell with phosphate maintained at pH 7.5 as a reference plan was used to analyze the damaged filtrate using an ultraviolet (UV) spectrophotometer at a repetition of 276 nm. The following examples were used to define the centralization of HCL Tamsulosin: 1 hour, 2 hours, 4 hours, 6 hours, 8 hours, 10 hours, 12 hours, 15 hours, 18 hours, and 24 hours, as well as the estimated rate of discharge. The distribution of all medications over time was plotted (Maclean, Armstrong et al. 2024).

2.15. Drug release kinetics

Drug release data were fitted into zero-order, first-order, Higuchi, and Korsmeyer-Peppas models to determine the release mechanism. Regression coefficients (R²) and release exponent (n) values were calculated to identify the best fit model and the type of release (Fickian or non-Fickian).

2.16. Zero-order kinetics

Plotting the overall proportion of drug release against time allowed for observation to determine both the slope and the value of the coefficient of correlation (Fard and Fard, 2021).

2.17. Hixson - Crowell model

The Hixson-Crowell shape root law is what determines this. Plotting the shape base of the medication's aggregate rate arrival versus time was done here. The diagram was decoupled from the relapsing line esteem (R2) and the rate steadiness of delivery (KHC). The equation was given below (Askarizadeh, Esfandiari et al. 2023).

 $Q0^{1/3} \ - \ Qt^{1/3} = K_{HC} \ t$

Q0 is the initial amount of the drug

Qt is the amount of drug released in time t

K_{HC} is the rate constant for the Hixson-Crowell rate equation

2.18. Korsemeyer-Peppas model

This fundamental analytical formula is used to describe the general solvent release behavior from regulated release polymer matrices. The graph indicates that the log of the total proportion of medications issued versus time, and the sloping logarithm has been used to obtain

the line of regression values (r2) and 'n'. The following equation is applied:

 $F = (Mt/M) = kt^n$

F is the Fraction of the drug released

Mt is the amount of drug released at time t

M is the total amount of drug in dosage form

k is the kinematic constant

t is the Discharge time

n is the diffusional exponent for drug release

2.19. Fourier Transform Infrared Spectroscopy (FTIR)

The purpose of this study is to verify whether the functional groups found in the polymers and monomers utilized in the formulations are present. All samples are thoroughly ground before the test examination, and the structure is assessed using the Bruker FTIR imaging spectrometer (the model Tensor 27, Germany) with attenuated total reflectance and Opus data collection software. The FT-IR spectra are examined at room temperature in the scanning range of 4000 to 600 cm⁻¹.

2.20. Thermo-gravimetric Analysis (TGA)

This study is being conducted for thermal analysis, which determines the mass of the designated samples over time as the temperature rises. This data examines physical and chemical characteristics such as phase transfer, adsorption, absorption, and solid thermal breakdown into a gas transition or reaction. The Q5000 series heat testing technique (TGA instruments, Western Sussex, UK) is employed for TGA analysis. The sample is heated in a nitrogen stream at a rate of 20 degrees Celsius per minute from 25 to 600 degrees Celsius (dry) in a pan containing 0.5 to 5 milligrams (Rojek, Bartyzel et al. 2024).

2.21. Differential scanning calorimetry (DSC)

DSC is a heat analytical technique that measures heat transport to or from a sample as an indicator of temperature or time. A highly efficient method is to assess the material's crystallization, basic heat energy, the temperature of glass change, melting point, oxidative behavior, and thermal stability (Gonzalez, Pena et al. 2022). A small quantity of 5–10 mg of the polymer cashew gum was added to the temperature-controlled DSC cell, in contrast to the formulation used for the DSC sample cell. The same method we used with Tamsulosin HCl and formulation. The sample must be heated or cooled at a continuous or regulated rate while the heat flow is managed in order to characterize the phase transition. TGA analysis is performed using the Q5000 setup, a heated examination system. A skillet containing 0.5 to 5 mg is linked to an analyzer, and the example is heated at a rate of 20 degrees Celsius per minute between 25 to 600°C in a dry nitrogen flood.

2.22. X-Ray Differential (XRD)

The Bruker D8 diffractometer (Germany) is used for this study at room temperature (Ainurofiq, Setianto et al. 2020). A Glass slide was taken, and the polymer, drug, and formulation were put on a tray to level the surface. Samples over 5 to 50 °C were studied using a piece of copper (K α radiation springs) with a wavelength of 1.542 and a slit size of 1 mm

2.23. Scanning Electron Microscopy (SEM)

Using an electron beam, an electron microscope creates an image of the sample's surface, providing information about its topography, including its crystalline and amorphous structure. The apparatus utilized to analyze the sample tablets was the SEM Quanta 400 (Cambridge, UK). By taking photomicrographs, the surface morphology of both the crushed and entire tablets was assessed (Gunawardana, Kong et al. 2023).

3. Results and discussion

3.1. Purification of cashew gum

The % yield was determined by weighing the dried, purified cashew gum after its purification. With a final output of 73.91%, the recovery rate from the raw plant exudate was found to be excellent. This high yield is in line with previous reports of yields from comparable extraction procedures in studies involving natural gum. It indicates that the purifying approach used in this investigation was practical. Afterwards, the gum that had been extracted was studied and used in the Tamsulosin HCl tablet formulation as a matrix polymer for sustained-release technology.

3.2. Physical testing of cashew gum

Cashew gum was physically tested by looking at its color, flavor, odor, and overall appearance. Table 2 displays the physical test outcomes. 2 also presents measures and discusses the moisture and insoluble matter contents of cashew gum (Silva, Oliveira et al 2024).

Table 2: Physical properties of the cashew gum

Property	Characteristics of cashew gum
Color	Yellowish, Glassy white
Taste	Bitter
Odor	Non order
Appearance	Smooth
Moisture	11.14 ± 0.24
Viscosity (0.50) % w/v	84.2 (cps)

3.3. Flow curves for cashew gum mucilage

By adding varying amounts of each gum into a viscometer for both the loading and the removal of the shear stress, flow curves were measured. Table 3 displays the shear stress results for cashew gum mucilage and xanthan gum mucilage, respectively, in a flow curve.

Table 3: Rheology of 10% w/v cashew gum

	Loading			Unloading		
Wt./g	Time /sec	Revs. /sec	Wt./g	Time /sec	Revs. /sec	
0	128.21	0.78	50	8.18	12.23	
5	66.23	1.51	40	10.05	9.95	
10	26.04	3.84	30	12.66	7.90	
20	19.84	5.04	20	19.46	5.14	
30	12.55	7.97	10	26.67	3.75	
40	9.85	10.15	5	69.93	1.73	
50	8.26	12.11	0	131.58	0.76	

3.4. Swelling capacity of cashew gum mucilage

To determine the capacity for swelling or swelling index, the gum was submerged in water, and its ability to swell over 24 hours was noted.

3.5. Flow properties of the gums

Calculations of the flux properties of cassava and xanthan gum were made using bulk mass and density. The flow characteristics of powder are studied by comparing the tapping density and bulk density (Ofori-Kwakye, Asantewaa et al. 2010). The details of the powder are provided below.

Number of tapping = 100 times

Hausner's ratio, Carr's index, and angles of repose are further metrics used to quantify flow characteristics. Table 4 displays the outcomes for flow properties obtained using various techniques.

Table 4: Bulk density of cashew gums

Sample	Initialvol (ml)	Tapped vol (ml)	Bulk density (Do)	Tapped density (Df)	HausnerHausner's Ratio	Carr's index (%)	Angle of repose
Cashew gum	17	16	0.59	0.63	1.07	6.35	24.67

3.6. Particle size analysis

Sampling was used to determine the size of particles and particle size distribution, and the results were reported..

3.7. Particle size distribution of cashew gum mucilage

To determine the particle's size and dispersion, 120 grams of cashew gum mucilage were employed. The effects of the cashew gum mucilage distribution on particle sizes are shown in Table 24.5 (Porto & Cristianini, 2014).

Table 5. Particle size distribution of cashew gum mucilage

Sieve no.	Aperture size (µm)	Range (µm)	Weight retained (g)	Weight retained (%)
60	2 50	250-425	1.98	1.65
80	180	180-250	4.45	3.71
200	75	75-180	95.12	79.27
Pan		<75	18.45	15.38

3.8. Flow properties of Tamsulosin HCl granules

The bulk and density ratios were used to calculate the granule flux characteristics. The fluidity of Tamsulosin HCl grains was also

determined using the angle of rest or the Hausner ratio. Table 6 displays the results for granular flow characteristics.

Table 6: Bulk density of Tamsulosin granules prepared

Batch No.	Bulk density (g/mL)	Tapped Bulk density (g/mL)	Hausner's ratio	Compressibility Index (%)	Angle of repose
1	0.56	0.59	1.05	5. 1	30.81 ± 0.007
2	0.45	0. 48	1.07	6. 3	33.42 ± 0.013
3	0.445	0.50	1.11	10	28.55 ± 0.026
4	0.50	0.53	1.06	5.7	31.50 ± 0.076
5	0.50	0.56	1.12	10.7	27.11 ± 0.113
6	0.48	0.50	1.04	4	35.30 ± 0.006
7	0.45	0.5	1.11	10	26.41 ± 0.017
8	0.50	0.56	1.12	10.7	29.60 ± 0.115
9	0.48	0.53	1.10	10.4	31.74
10	0.53	0.59	1.11	10.2	30.20 ± 0.010

3.9. Compression of Tamsulosin HCl matrix tablets

The granules were compressed into tablet form to create Tamsulosin HCl matrix tablets. The following details pertain to the compression for matrix tablets.

Tablet weight = 420 mg Number of tablets = 80 per batch (15 batches in all) Practical yield = 958 tablets

3.10. Quality control tests carried out on matrix tablets 3.10.1. Uniformity of Weight

A weight uniformity test was performed on the tablets (Table 7) to determine how much each one differed from the average weight. Using the following formula, the percentage variations of the tablet from the mean were determined by use of the following formula:

Table 7: Uniformity of weight of the batches of Tamsulosin matrixtablets

% deviation = $\underline{A - B} \times 100$,

Where A is the initial weight of tablets, and B is the average weight of 20 tablets

Batch No.	Total tablet weight (g)	Average weight $(g) \pm SD$	Max % deviation	Inference
1	8.82	0 .442 ± 0.013	4.834	PASS
2	8.67	0.434 ± 0.008	2.978	PASS
3	8.34	$0.4178 \pm\ 0.012$	4.894	PASS
4	8.56	0.429 ± 0.010	4.022	PASS
5	8.57	0.428 ± 0.012	4.53	PASS
6	8.51	0.425 ± 0.011	4.373	PASS
7	8.39	0.419 ± 0.012	3.674	PASS
8	8.49	$0.424 \pm\ 0.011$	4.689	PASS
9	8.56	$0.428 \pm\ 0.012$	4.139	PASS
10	8.35	0.417 ± 0.010	4.364	PASS

3.11. Crushing strength (Hardness)

By applying force till the tablets broke, the hardness of the tablet was used to measure its strength or crushing strength. Table 8 presents the findings on tablet hardness (Khan, 2021).

Table 8: Crushing strength of Tamsulosin HCl matrix tablets

Batch Number	Mean force applied (Kg)
1	4.5 ± 1.12
2	$6.9~\pm~1.61$
3	$3.8~\pm~0.76$
4	$4. \ 0 \ \pm \ 0.82$
5	$4.0~\pm~0.78$
6	4.1 ± 1.23
7	$4.1 ~\pm~ 0.66$
8	$4.4~\pm~0.65$
9	$5.3 ~\pm~ 1.19$
10	$4.1~\pm~0.84$

3.12. Friability

The method for determining the friability of tablets involves weighing 10 tablets before and after the revolutions, then dividing the result by

the beginning weight multiplied by 100, as shown in Table 9 (Zomenko, Gubenia et al. 2024).

Table 9: Friability of the Tamsulosin HCl matrix tablets

Batch	Initial weight	Final wt.	Weight loss	% loss
	(W_i)	(W_f)		
1	6.02	5.95	0.07	1.00
2	6.29	6.27	0.02	0.17
3	6.29	6.24	0.05	0.65
4	6.37	6.29	0.08	1.11
5	6.36	6.30	0.06	0.78
6	6.37	6.33	0.04	0.48
7	6.32	6.30	0.02	0.17
8	6.30	6.24	0.06	0.81
9	6.37	6.32	0.05	0.64
10	6.20	6.11	0.09	1.31

3.12. Swelling index of Tamsulosin HCl matrix tablets

Table 10 displays the measured swelling index for Tamsulosin HCl matrix tablets across all batches (Markl, Maclean et al. 2021).

Table 10: Thickness of the Tamsulosin HCl matrix tablets

				% W	ATER ABS	ORBED				
Time(hr)	B.1	B.2	B.3	B. 4	B. 5	B. 6	B.7	B.8	B. 9	B. 10
0.08	4.7	28.6	7.1	11.9	11.4	6.8	21.4	22.5	16.7	25.0
0.25	11.6	54.8	7.1	11.9	6.8	11.4	38.1	32.5	23.8	61.4
0.50	4.7	85.7	0.0	0.0	0.0	11.4	57.1	57.5	26.2	79.5
1.00	0.0	92.9	0.0	0.0	0.0	2.3	66.7	60.0	19.0	93.2
2.00	0.0	116.7	0.0	0.0	0.0	0.0	90.5	67.5	9.5	118.2
4.00	0.0	150.0	0.0	0.0	0.0	0.0	111.9	77.5	0.0	152.3
6.00	0.0	190.5	0.0	0.0	0.0	0.0	140.5	62.5	0.0	184.1
8.00	0.0	242.9	0.0	0.0	0.0	0.0	159.5	55.0	0.0	197.7
10.00	0.0	269.0	0.0	0.0	0.0	0.0	178.6	35.0	0.0	211.4
12.00	0.0	285.7	0.0	0.0	0.0	0.0	223.8	0.0	0.0	236.4
15.00	0.0	288.1	0.0	0.0	0.0	0.0	231.0	0.0	0.0	250.0
18.00	0.0	285.7	0.0	0.0	0.0	0.0	235.7	0.0	0.0	250.0

3.13. Assay of Tamsulosin HCl matrix tablets

By measuring the absorption of Tamsulosin HCl at various concentrations, the amount of Tamsulosin HCl in the pill form is ascertained. To produce an auto-zero for the construction of the Tamsulosin HCl calibration curve, 0.1 M NaOH is used as a blank at 276 nm.

Table 11 below displays the absorptions of various Tamsulosin HCl concentrations. Crushed tablets are filtered before absorption is measured in order to perform the Tamsulosin HCl tablet assay. Table 11 displays the matrix tablet assays (Khashaba, Abdelgaleel et al. 2022).

Table 11: Shows the drug release characteristics over time for several standard reference (Maxflow capsule) tablets.

BatchNo	Expectedweight(g)	Actual weight(g)	Conc (%w/v)	AverageAbs	A (1% 1 cm)	Assay(%)
1	0.4407	0.4410	0.002001	0.660	329.776	101.5 ±0.408
2	0.4332	0.4332	0.002000	0.641	320.500	98.7 ± 0.510
3	0.4168	0.4164	0.001998	0.645	322.810	99.4 ± 0.205
4	0.4278	0.4275	0.001999	0.647	323.727	99.7 ± 0.510
5	0.4282	0.4279	0.001999	0.646	323.226	99.5 ± 0.249
6	0.4254	0.4256	0.002001	0.654	326.846	$100.6{\pm}0.566$
7	0.4194	0.4193	0.002000	0.649	324.577	99.9 ± 0.216
8	0.4244	0.4242	0.001999	0.645	322.652	99.3 ± 0.170
9	0.4276	0.4275	0.002000	0.642	321.075	$98.9 \pm\! 0.249$
10	0.4171	0.4173	0.002001	0.647	323.345	99.5 ± 0.170
Pure sample	0.1000	0.1002	0.002004	0.651	324.850	

 Table 12: Drug release profile of reference standard (Maxflow capsule)

Time/hr.	Mean absorbance	Conc.(%w/v)	% release
0.083	0.258	0.00883	8.83 ± 0.056
0.25	0.327	0.01072	10.71 ± 0.052
0.5	0.633	0.01913	19.13 ± 0.018
1	0.819	0.02434	24.34 ± 0.003
2	1.053	0.03091	30.91 ± 0.012
4	1.377	0.039945	39.95 ± 0.013
6	1.623	0.04707	47.07 ± 0.006
8	1.979	0.05718	57.18 ± 0.014
10	2.142	0.06219	62.19 ± 0.005
12	2.315	0.067445	67.45 ± 0.006
15	2.664	0.07756	77.56 ± 0.008
18	2.674	0.07868	78.68 ± 0.007
21	2.777	0.08229	82.29 ± 0.011
24	2.766	0.08275	± 0.011

3.14. Mechanism and release kinetics of Tamsulosin HCl matrix tablets

Numerous phases of drug release from matrix tablets were investigated in Figs 1 and 2, and statistics on drug release from matrix tablets were developed in the form of time-series kinetics. The impact of kinetics on drug release is seen in Table 13 (Assaf, Ghanem et al. 2022).

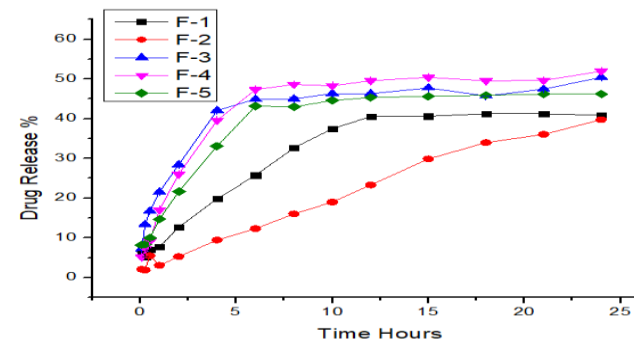


Figure 1. Drug release profiles of formulations F-1 to F-5 over 24 hours

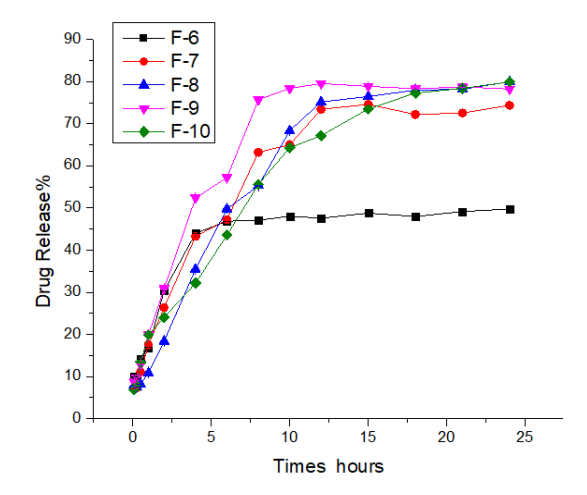


Figure 2: Drug release profiles of formulations F-6 to F-10 over 24 hours

Table 13: Mechanism and release kinetics of the Tamsulosin HCl matrixtablets

Batch No.	Zero Order		First Order		Higuchi		Hixson-Crowell	
	Ko	R^2	\mathbf{K}^{1}	\mathbb{R}^2	KH	R^2	KHC	R ²
1	0.0278	0.8107	0.0006	0.7088	1.2050	0.9325	0.0012	0.748
2	0.0273	0.9880	0.0009	0.8257	1.0842	0.9563	0.0015	0.909
3	0.0237	0.5265	0.0004	0.4700	1.1279	0.7310	0.0009	0.498
4	0.0298	0.6313	0.0005	0.5209	1.3794	0.8308	0.0011	0.562
5	0.0268	0.6664	0.0005	0.5854	1.2228	0.8542	0.0010	0.615
6	0.0257	0.5913	0.0004	0.5221	1.2023	0.7952	0.0009	0.547
7	0.0493	0.7735	0.0006	0.6305	2.1720	0.9231	0.0015	0.687
8	0.0568	0.8392	0.0007	0.7080	2.4360	0.9493	0.0017	0.757
9	0.0507	0.6997	0.0006	0.5969	2.2861	0.8753	0.0015	0.637
10	0.0535	0.8816	0.0006	0.7068	2.2722	0.9750	0.0016	0.779

3.15. Fourier Transform Infrared Spectroscopy (FTIR)

Drug-polymer interactions, as well as linkages in the functional groups they form, are ascertained using FTIR. Figures 3, 4, and 5 show the FTIR spectra of the cashew gum drug and formulation, respectively. Polymer's infrared spectra show a strong broad peak of O-H (carboxylic acid) or conjugated -CH₂ groups stretching at 3050 cm⁻¹. At . Atof 1470 cm⁻¹, there is another high peak at 1801 cm⁻¹ due to the presence of C=O (ester), and at 1195 cm⁻¹ due to the C-O stretching (Amornrojvaravut et al. 2023)

Figure 3 displays the FTIR spectrum of the active medications, cashew gum. The carboxyl gathering caused the trademark tops to appear at 1750 cm $^{-1}$, the essence of the C–O stretch at 1086 cm $^{-1}$, the C = C (fragrant expanding) at 1500 cm $^{-1}$ in slight movement, the – CH3 twist at 1470 cm $^{-1}$, and the existence of O–H (carboxylic acids) at 2990 cm $^{-1}$. Drug FTIR range showed a curve at 2990 cm $^{-1}$ due to a slight move that changed the essence of the O–H (carboxylic corrosive) transition, at 1420 cm $^{-1}$ due to -CH3 twist, and at 1670 cm $^{-1}$ due to the existence of C = O (ester).

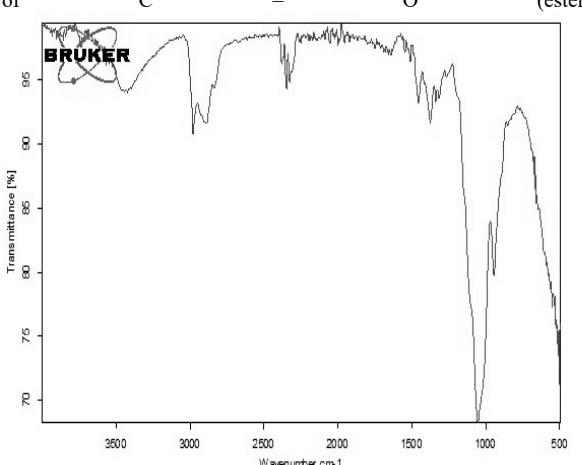


Figure 3: FTIR spectra of cashew gum

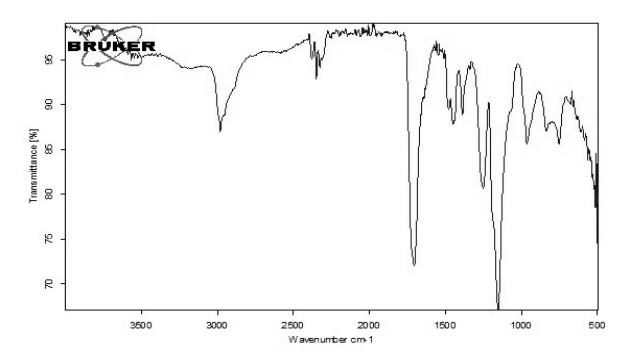


Figure 4: FTIR spectra of the drug

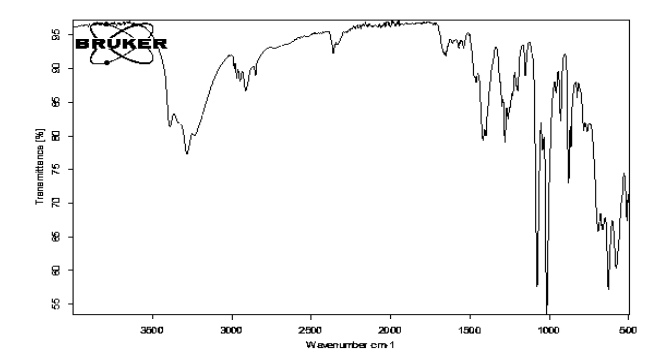


Figure 5: FTIR spectra of the formulation.

3.16. Thermogravimetric Analysis (TGA)

The use of a Thermogravimetric Analyzer was used to perform a thermogravimetric analysis (TGA) at a rate of 25 ml/min of nitrogen and a warming rate of 10 °C/min between 20 and 500 °C. The TGA graph of cashew gum, shown in Figure. 5, shows that, similar to DSC, the dehydration phase occurs above 100 °C with a weight loss 1%. After 300 °C, the polymer begins to decompose, and at around 350 °C, 95.2% of the polymer is decomposed. Similar to this, TGA

of polymer reveals a 6.5% weight loss as a result of dehydration, almost at 110 °C, and polymer breakdown beginning at 300 °C. The medicine is stable according to the TGA for the formulation, with 50% breakdown occurring at 300 °C with 98% decomposition occurring at 350 °C or higher (Fig 6). The composition is more stable in TGA as shown in Fig 7 and 8, with a 9% weight loss percentage at 100 °C from moisture, 60% weight loss at the endothermic peak at 300 °C, and 88% weight reduction at 400 °C or higher.

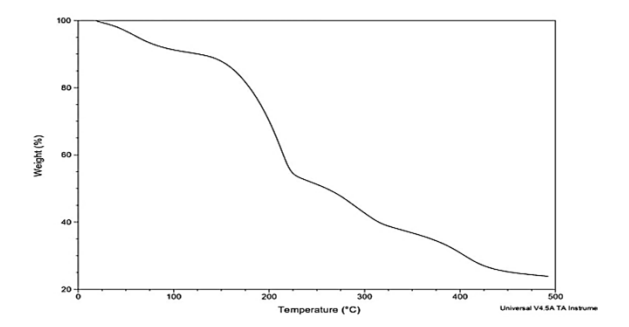


Figure 6: Thermo-gravimetric analysis of cashew gum

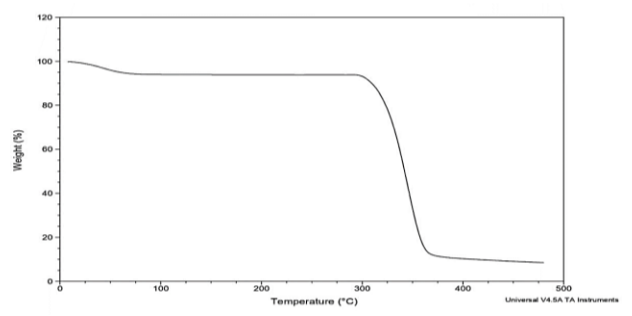


Figure 7: Thermo-gravimetric analysis of the drug

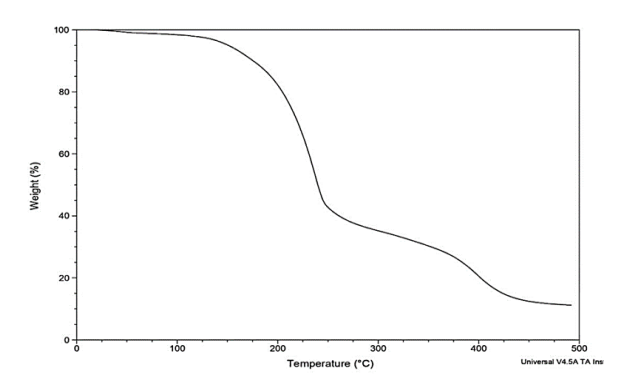


Figure 8: Thermo-gravimetric analysis of the given formulation

3.17. Differential scanning calorimetry

Cashew gum, drug, and formulation polymer DSC thermograms are compared to the formulation. Figure 8 shows that the polymer has three endothermic peaks. The first peak, which occurred between 50 °C and 55°C, indicated the temperature at which the glass transition or weight loss due to moisture evaporation and other volatile components occurred. The next minor endothermic peak, which occurred at 175°C and was followed by an exothermic peak, indicated the denaturing or breakdown of the polymer. Since the polymer is amorphous, Fig. 9 displays two broad endothermic peaks at 95°C and 274.3°C for the polymer. The first endothermic peak indicates the polymer's glass transition temperature, while 250.4 indicates melting or degradation.

The formulation's DSC thermogram (Figs 10 and 11) displays two endothermic peaks at 150.5 and 275.5, indicating that the composition is more stable when degradation and decomposition occur at higher temperatures. This results in two endothermic peaks at 150.5 and 275.5, indicating that the composition is more stable when degradation and decomposition are shifted towards higher temperatures, resulting in a more stable product.

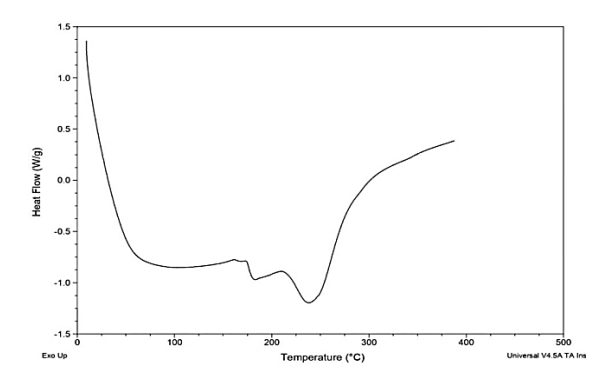


Figure 9: DSC analysis of the given cashew gum

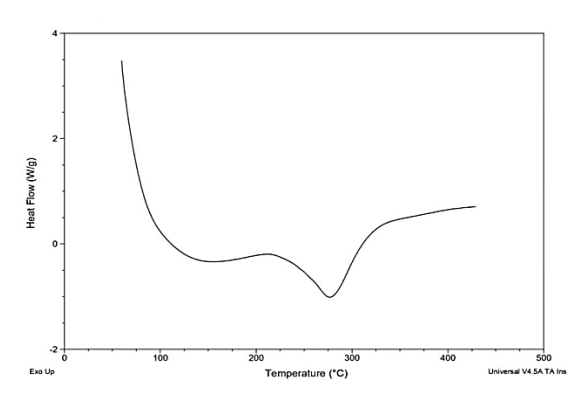


Figure 10: DSC analysis of the given drug

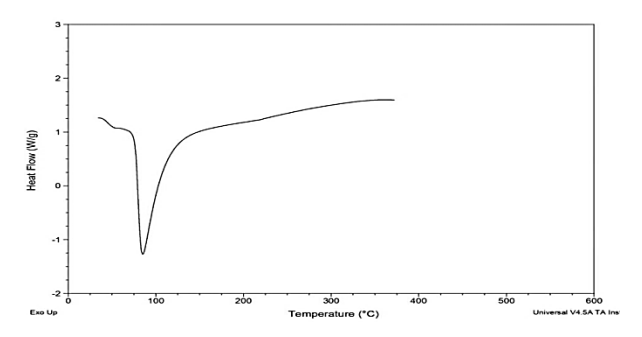


Figure 11: DSC analysis of the given formulation

3.18. X-Ray Differential XRD

It is essential to determine the crystalline and amorphous structures of the formulation, as they impact the drug's solubility and release through the formulation. Peak. The strong peak represents the crystalline structure of the polymers utilized in the formulation. The strong peak represents the crystalline structure of the polymers utilized in the formulation. The strong peak represents the crystalline structure of the polymers utilized in the formulation. The strong peak represents the crystalline structure of the polymers used in the formulation, which the polymer produces in Fig. 12 at two distinct angles, $\theta = 12.1^{\circ}$ and

 15.1° , respectively. The drug XRD in Figure 13 does not show a distinct peak at the O2 θ angle. Similarly, the tablet formulation's structure is depicted in Figure 14. Fourteen is more amorphous in character, and the XRD graph of the formulation shows a little shift (Munnangi, Narala et al. 2024).

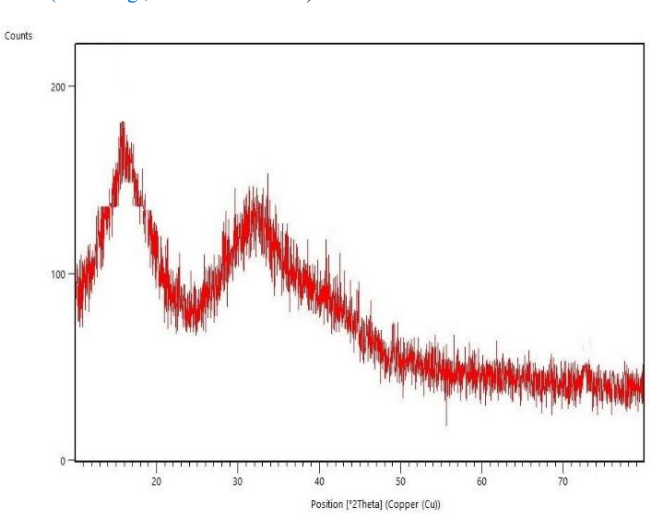


Figure 12: XRD of cashew gum

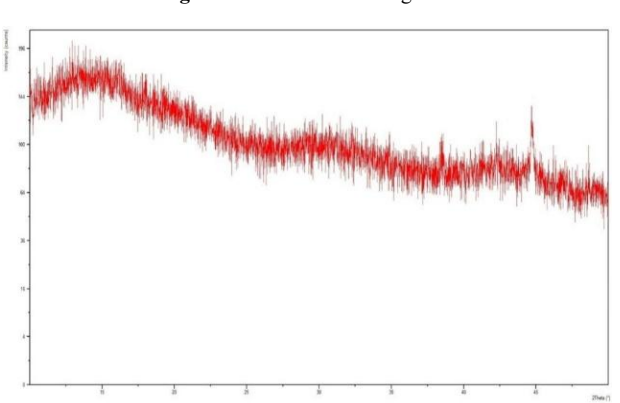


Figure 13: XRD of the drug

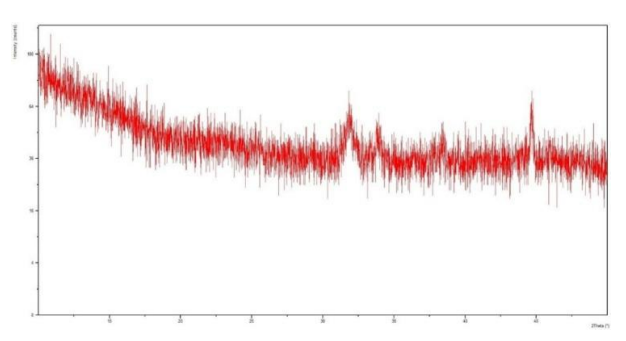


Figure 14: XRD of formulation

3.19. Scanning Electron Microscopy SEM

In Figures 15 and 16, the tablet formulation is examined at various magnification levels, such as 500 μm and 400 μm , to ascertain the surface shape of the tablet or crushed tablet. The tablet's porous structure can be seen in the figures. The tablet's shape indicates that the granules have better disintegration qualities and are more soluble.

Figure 15 shows the SEM analysis of tablets, and Figure 16 shows the SEM of tablet powder (Tayyab, Mahmood et al. 2022).

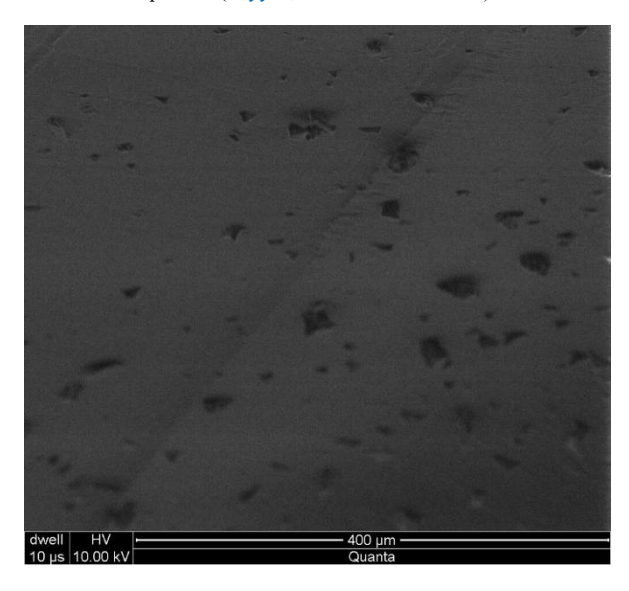


Figure: 15 SEM of tablet

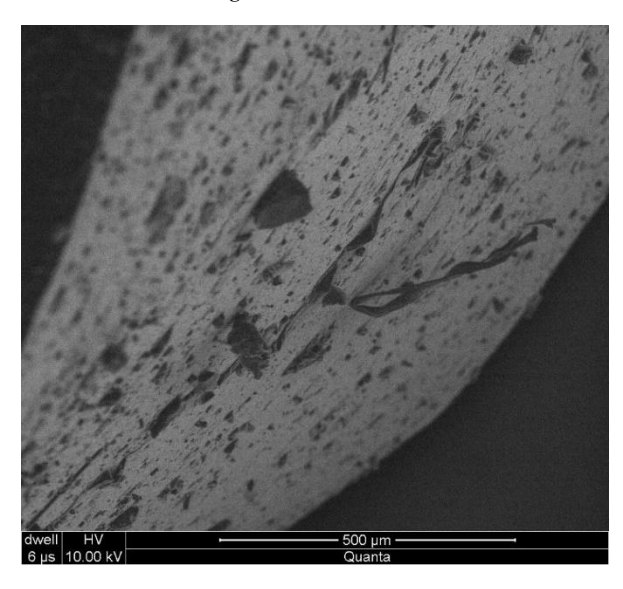


Figure 16: SEM of tablet powder

3.Conclusion

This creative effort resulted in the formulation of the following conclusive points. Cashew gum may be distilled to guarantee a respectable yield. The gums of cashew and xanthan both exhibited pseudoplastic flow. The consistency of the substance and the weight tests were both successful for both tablets. Both tablet batches passed a crushing power test (Bar Batch 3). All tablet sets passed the friability test, which was conducted on bar batches 4 and 10. Tablets containing just xanthan gum had the and most significant concentrations of the compressive force friction ratio (CSFR) as a modification of the escape. The tablets in batches two and three showed the highest and lowest swelling indices, respectively.

The study showed that the use of cashew with xanthan gums alone is insufficient to control medication release. Similar to the studies in

Batches 10, 11, and 12, the mixture containing cashew gums and xanthan demonstrated good sustained release characteristics. In contrast, the Maxflow Tablet and other medications may continue to be released from batches 13 to 15 for all three varieties. The medicine Gonzalez, R., M. Á. Pena, N. S. Torres and G. Torrado (2022). "Design. might have been administered using the Higuchi model of pharmaceutical energy because the release profile fits the Higuchi equation better than the other components. The drug is discharged through irregular or non-Fickian dispersion after the delivery type 'n' Gopaiah, V. (2022). "Formulating & evaluating oral sustained-release was determined to be between 0.45 and 0.89.

Declarations

Ethics approval and consent to participate

Not applicable.

Ethical consideration

Not applicable.

Consent for publication

Not applicable.

Competing interests

The authors declare that they have no competing interests

Acknowledgements

Not applicable.

Author's Contribution

Conceptualization, writing the original draft: Kashif Barkatu, Umair IKram Dar. Formal analysis, investigations, and funding acquisition: Anaum Asghar, Hira Shahid, Nariman Shahid. Resources, project administration, reviewing and editing, data validation: Rabia Arshad, Zeeshan Akbar, Shamsha Kanwal. Data curation, supervision: Hamza Rafeeq, Haroon Yousaf

Funding

This work received no external funding.

Data Availability

The data used in this study are included in the article

- Aboul-Enein, H. Y., R. F. Hussein, M. A. Radwan, A. Yusuf, W. Al-Ahmadi and S. Al-Rawithi (2003). "Tamsulosin dissolution from pharmaceutical dosage forms using an automated HPLC system." Journal of liquid chromatography & related technologies 26(7): 1109-1116. crossref
- Ainurofiq, A., A. B. Setianto, Y. P. Nugraha, V. Suendo, H. Uekusa and S. N. Soewandhi (2020). "X-ray diffraction and vibrational spectroscopic studies of the intermolecular interactions on the grinding and compaction behaviours of lopinavir and ritonavir crystals." Acta Poloniae Pharmaceutica-Drug Research 77(2): 259-269. DOI: crossref Maclean, N., J. A. Armstrong, M. A. Carroll, M. Salehian, J. Mann, G.
- Amornrojvaravut, C. and J. Peerapattana (2023). "Application of coprecipitated glutinous rice starch as a multifunctional excipient in direct compression tablets." Helivon 9(9). crossref
- Askarizadeh, M., N. Esfandiari, B. Honarvar, S. A. Sajadian and A. Azdarpour (2023). "Kinetic modeling to explain the release of medicine from drug delivery systems." ChemBioEng Reviews 10(6): 1006-1049. crossref
- Assaf, S. M., A. M. Ghanem, S. a. A. Alhaj, E. A. Khalil & A. A. Sallam (2022). "Formulation and evaluation of Eudragit® RL polymeric double layer films for prolonged-release transdermal delivery of tamsulosin hydrochloride." AAPS PharmSciTech 23(6): 210.crossref
- Fard, A. M. and M. M. Fard (2021). "Modeling drug release." Eurasian J Sci Tech 1(1): 284-301. crossref
- Fosu, M.-A., K. Ofori-Kwakye, N. Kuntworbe and M. A. Bonsu (2016). "Investigation of blends of cashew and xanthan gums as a potential

- carrier for colonic delivery of Ibuprofen." International Journal of PharmTech Research 9(7): 369-38 0
- development, and characterization of amorphous rosuvastatin calcium tablets." PLoS One 17(3): e0265263. crossref
- diclofenac sodium tablets by using xanthan and cashew gums." Journal of Case Studies and Case Reports: 34-41.ref
- Gunawardana, C. A., A. Kong, D. O. Blackwood, C. T. Powell, J. F. Krzyzaniak, M. C. Thomas and C. C. Sun (2023). "Magnesium stearate surface coverage on tablets and drug crystals: Insights from SEM-EDS elemental mapping." International journal pharmaceutics 630: 122422. crossref
- Holanda, V. A., M. C. Oliveira, C. I. de Oliveira Torres, C. de Almeida Moura, H. Belchior, E. D. da Silva Junior and E. C. Gavioli (2024). "The alpha1A antagonist tamsulosin impairs memory acquisition, consolidation and retrieval in a novel object recognition task in mice." Behavioural brain research 469: 115027. crossref
- Kava BR, Verbeek AE, Wruck JM, Gittelman M. Tamsulosin dispensation patterns in the United States: a real-world, longitudinal, population claims database analysis. Transl Androl Urol. 2019;8(4):329-338. doi:crossref
- Khan, A. (2021). "Prediction of quality attributes (mechanical strength, disintegration behavior and drug release) of tablets on the basis of characteristics of granules prepared by high shear wet granulation." Plos one 16(12): e0261051. crossref
- Khashaba, P. Y., M. Abdelgaleel, S. M. Derayea and D. M. Nagy (2022). "Development of a simple validated spectrofluorometric method for the assay of midodrine in tablets dosage form; Application to content uniformity testing." Spectrochimica Acta Part A: Molecular and Biomolecular Spectroscopy 273: 121046. crossref
- Kumar, A., A. Moin, A. Ahmed and H. G Shivakumar (2012). "Cashew gum a versatile hydrophyllic polymer: a review." Current Drug Therapy 7(1): 2-12.crossref
- Reynolds, B. Johnston and D. Markl (2024). "Flexible modelling of the dissolution performance of directly compressed tablets." International Journal of Pharmaceutics 656: 124084. crossref
- Malabadi, R. B., K. Kolkar and R. Chalannavar (2021). "Natural plant gum exudates and mucilage: pharmaceutical updates." Int J Innov Sci Res Rev 3(10): 1897-1912.ref
- Markl, D., N. Maclean, J. Mann, H. Williams, A. Abbott, H. Mead and I. Khadra (2021). "Tablet disintegration performance: effect of compression pressure and storage conditions on surface liquid absorption and swelling kinetics." International Journal of Pharmaceutics 601: 120382.crossref
- McVary, K. T., Roehrborn, C. G., Avins, A., et al. "Benign Prostatic Hyperplasia: Epidemiology and Comorbidities." The Journal of Urology, vol. 192, no. 5, 2014, pp. 1497-1507ref
- Munnangi, S. R., N. Narala, P. Lakkala, S. K. Vemula, S. Narala, L. Johnson, K. Karry and M. Repka (2024). "Optimization of a Twin

- screw melt granulation process for fixed dose combination immediate release Tablets: Differential amorphization of one drug and crystalline continuance in the other." *International Journal of Pharmaceutics* **665**: 124717. crossref
- Nanjwade, B., M. Ali, V. Nanjwade and F. Manvi (2010). "Effect of compression pressure on dissolution and solid state characterization of cefuroxime axetil." J. Anal. Bioanal. Tech 1(3): 1-6. doi:crossref
- K. Ofori-Kwakye, E. Obese, M. E. Boakye-Gyasi. (2013). Formulation and In-vitro evaluation of sustained release diclofenac sodium matrix tablets using blends of cashew gum, xanthan gum and hydroxypropylmethylcellulose as hydrophilic drug release modifiers. *Indian Journal of Novel Drug Delivery* 5(4), 187-197<u>ref</u>
- Ola, O. O., Emikpe, B. O., Kuntworbe, N., Michael, O. A., Jarikre, A. T., Onilude, M. O., Asantewaa, Y. O., & Asare, A. D. (2024). Evaluating cashew tree gum as a potential vaccine carrier: purification, phytochemical analysis and biocompatibility assessment. *Tropical Journal of Natural Product Research*, 8(9), 8447-8452 crossref
- Pawar, R., M. Jaimini, B. S. Chauhan and S. K. Sharma (2014). "Compression coated tablets as drug delivery system (tablet in tablet): a review." *International Journal of Pharmaceutical Research and Development* 6(1): 21-33.ref
- Porto, B. C. and M. Cristianini (2014). "Evaluation of cashew tree gum (Anacardium occidentale L.) emulsifying properties." LWT-Food Science and Technology 59(2): 1325-1331. crossref
- Rivera-Navarro, J. C., M. Y. M. Pizaño, S. L. Martínez-Hernández, J. Ventura-Juárez, D. Ibarra-Martínez and M. H. Muñoz-Ortega (2024). "effects of the adrenergic blockers tamsulosin and carvedilol on the homeostasis of the endoplasmic reticulum of liver cells. " World Journal of Pharmaceutical Science and Research 3 (2).38-53.ref
- Rojek, B., A. Bartyzel, W. Sawicki and A. Plenis (2024). "DSC, TGA-FTIR and FTIR assisted by chemometric factor analysis and PXRD in assessing the incompatibility of the antiviral drug arbidol hydrochloride with pharmaceutical excipients." *Molecules* 29(1): 264. crossref
- Silva, T. M., A. C. D. J. Oliveira, A. D. Leão, R. K. L. G. Ramos, L. L. Chaves, E. C. da Silva Filho, M. F. d. L. R. Soares and J. L. S. Sobrinho (2024). "Cashew gum as future multipurpose biomacromolecules." Carbohydrate Polymers: 122749.crossref
- Tafere, C., Z. Yilma, S. Abrha and A. Yehualaw (2021). "Formulation, in vitro characterization and optimization of taste-masked orally disintegrating co-trimoxazole tablet by direct compression." *PloS one* 16(3): e0246648. crossref
- Tayyab, A., A. Mahmood, H. Ijaz, R. M. Sarfraz, N. Zafar and Z. Danish (2022). "Formulation and optimization of captopril-loaded microspheres based compressed tablets: in vitro evaluation." International Journal of Polymeric Materials and Polymeric Biomaterials 71(4): 233-245. crossref
- Zomenko, O., O. Gubenia, O. Chepeliuk and D. Herasymenko (2024). "Effect of compression modes on tablet strength and friability." *Ukrainian Journal of Food Science* 12(1). crossref